Rapid Histone Post-Translational Modification Analysis Using Alternative Proteases and Tandem Mass Tags.

Natalie P. Turner [1], Sabyasachi Baboo [1], Patrick Garrett [1], Jolene K. Diedrich [1,2], Michael Bajo [3], Marisa Roberto [3], and John R. Yates III [1]*.

[1] The Scripps Research Institute, Department of Integrative and Structural Computational Biology, 10550 North Torrey Pines Rd, La Jolla, CA 92037, United States of America

[2] The Scripps Research Institute Multi-Omics Core Facility, 10550 North Torrey Pines Rd, La Jolla, CA 92037, United States of America

[3] The Scripps Research Institute, Department of Translational Medicine, 10550 North Torrey Pines Rd, La Jolla, CA 92037, United States of America

*Corresponding author: jyates@scripps.edu

Abstract

Histone post-translational modifications (PTMs) alter chromatin dynamics and contribute to the regulation of gene expression in health and disease. Mass spectrometry-based analysis is the gold-standard for histone PTM analysis, but it remains constrained by inefficient sample preparation workflows requiring multiple days. Here, we develop RIPUP (*R*apid *I*dentification of histone *P*TMs in *U*nderivatized *P*eptides), a streamlined multi-protease workflow that reduces sample preparation from days to hours while improving PTM coverage and quantitative accuracy. Through systematic evaluation of the Arg-C Ultra protease and a prototype recombinant (r)-Chymotrypsin protease under varied conditions, such as chemical derivatization using propionic anhydride and tandem mass tags (TMT), we demonstrated that Arg-C Ultra with TMT labeling achieves a detection of total PTM comparable to conventional Trypsin-based approaches. Using the HiP-Frag computational framework for unrestrictive PTM identification, we discovered that TMT's tertiary amine provides charge compensation that rescues the ionization of negatively charged acylations revealing 50 succinylation and 27 glutarylation sites – a 'dark epigenome' largely undetected by propionylation-based methods. We demonstrated that complementary digestion with Arg-C Ultra and r-Chymotrypsin provides orthogonal sequence coverage, enabling detection of PTMs in H2A variants, linker histones, and regions poorly represented by arginine-specific cleavage alone. Application of RIPUP to frozen-thawed rat hippocampal sections within a 3-hour workflow identifies >200 PTMs including biologically critical PTM sites H3 K27/K36/K37 methylation, H4 N-terminal acetylation patterns, and H2A ubiquitination at K118/K119. This rapid, high-efficiency platform enables timely discovery of epigenetic mechanisms and accelerates the path from PTM identification to therapeutic target validation.

Background

Mass spectrometry (MS)-based proteomics is a popular and powerful tool for analyzing histone post-translational modifications (PTMs), known as the 'histone code' [1,2]. Histone proteins assemble as octamers comprised of two copies of histone H2A, H2B, H3 and H4 to form the nucleosome core, which is sequentially wrapped in ~146-147 bp DNA during nucleosome assembly [3]. Tightly wound nucleosomes form chromatin, the major structural unit of chromosomes. Fundamental aspects of epigenetic regulation are under the control of 'writers' and 'erasers' that add and remove chemical groups (PTMs) to histones. These changes control gene transcription by altering chromatin structure and thus the accessibility of transcriptional machinery to chromatin. Histone PTM research has focused on understanding nuanced epigenetic mechanisms implicated in health and disease paradigms, including cancer [3], neurobiology [4], addiction [5], and the gut microbiome [6].

Garcia et al. first described a workflow that significantly advanced the field of histone PTM analysis by MS in 2007 [2]. As histones are lysine (K)- and arginine (R)-rich, traditional bottom-up proteomics with Trypsin cleavage produces mostly short peptides that are not within the appropriate mass or retention time range for detection by liquid chromatography-tandem mass spectrometry (LC-MS/MS). Hence, Garcia et al. (2007) [2] designed a workflow that includes a chemical derivatization step to propionylate ε-amino groups of lysine (K). This modification prevents Trypsin cleavage after K, generating longer, more hydrophobic peptides which improves solid-phase retention and chromatographic separation [2,7]. These tryptic peptides contain R as the C-terminal amino acid and produce stable, singly charged *y*-ion series fragments. While this workflow has undergone multiple iterations since its initial publication [7,8], alternative proteases and the optimization of parameters that may improve workflow efficiency, peptide sequence coverage, identify novel PTMs, improve reproducibility, or lower peptide coefficients of variation (CVs) is still relatively under-explored [9].

Two new-to-market enzymes – a prototype recombinant (r)-Chymotrypsin and Arg-C Ultra (Promega™) – offer significant advantages to the standard Trypsin and propionylation approach for histone PTM analysis by MS-based proteomics. For example, Trypsin digestion of histone proteins labeled with propionic anhydride should produce an Arg-C Ultra-like cleavage pattern (cleavage at the C-terminus of arginine), but labeling efficiency can be user-dependent and is prone to variability [10,11], which reduces the overall number of peptides that can be reliably used for quantitation. Additionally, r-Chymotrypsin and Arg-C Ultra require shorter incubation times (2 h compared to >6 h with Trypsin). Importantly, if derivatization is preferred for its chromatographic benefits, propionylation is required after digestion only to label unmodified lysines and peptide N-termini, as neither Arg-C Ultra nor r-Chymotrypsin cleaves at the lysine C-terminus, so that the cleavage specificity of the proteases is unaffected by lysine modification status. In contrast to standard Chymotrypsin, the prototype r-Chymotrypsin does not cleave after tryptophan (W) and shows increased specificity for leucine (L), tyrosine (Y), and phenylalanine (F), generating peptides not seen with Trypsin and Arg-C Ultra digestion, thus capturing different segments of histone protein sequences. These changes to the established protocol [1,2] can significantly reduce the overall sample preparation time for development of high-throughput workflows and reveal insights into histone PTMs not seen with Trypsin digestion [9].

While elimination of the propionylation step reduces overall sample preparation time, addition of propionyl groups to tryptic peptides increases their overall hydrophobicity, which is advantageous for retention of short, hydrophilic

peptides. However, separating peptidoforms with isobaric PTMs, similar retention times or small mass differences remains a challenge regardless of whether or not they are propionylated. Other approaches for labeling histone peptides have been reported, including recent work by Ryzhaya et al., which demonstrated that the Arg-C Ultra protease, which has substantially better arginine-cleavage specificity and efficiency than conventional Arg-C, can be combined with peptide-level derivatization using trimethylacetic anhydride (TMA) to reduce histone sample preparation time to ~3-4 hours [9]. Interestingly, tandem mass tags (TMT) [12] is a well-established amine-reactive label that has not been systematically evaluated for histone PTM analysis. TMT-labeling adds isobaric tags to primary amines, such as those of post-digestion peptide N-termini and unmodified K residues. Like propionyl labeling, TMT labeling creates peptides that are more hydrophobic, but with potentially higher labeling efficiency in a single one-hour incubation step. Importantly, the unique chemical structure of TMT, which includes a tertiary amine within the reporter region, may confer previously unrecognized advantages for detecting specific PTM classes that reduce the overall charge state of the peptide, such as negatively charged acylations, succinylation and glutarylation [13,14]. Additionally, TMT is compatible with multiplexed data acquisition and may offer benefits for quantitative analysis.

Recent advances in computational mass spectrometry have revealed that the histone PTM landscape is substantially more complex than previously appreciated. Vai et al. (2025) [15] recently developed HiP-Frag, an unrestrictive search workflow that identified 60 previously unreported modifications on core histones and 13 on linker histones across multiple cell lines and tissue samples. Their work demonstrated that rigorous computational filtering at the peptide-to-spectrum match (PSM) and peptide levels coupled with detailed mass offset search, rather than exhaustive validation using synthetic peptides, can enable confident discovery of novel PTMs at scale, expanding our understanding of the histone code beyond classical acetylation and methylation. However, while these computational advances have revealed the existence of numerous uncommon modifications, the key question of whether different sample preparation and chemical labeling strategies preferentially detect certain PTM classes remain unaddressed and has implications for potentially biasing our view of the epigenetic landscape. This consideration is particularly important given that propionylation neutralizes positive charges on lysine residues, which may affect the ionization efficiency of peptides bearing negatively charged modifications.

To address these challenges, we performed a comprehensive systematic evaluation of both the standard Trypsin protocol [1] and two alternative proteases, Arg-C Ultra and a commercially available prototype recombinant (r)-Chymotrypsin (Promega™), under multiple experimental conditions using histones extracted from HEK293T cells. We tested each protease with and without propionylation, under denaturing and non-denaturing conditions, generating 10 distinct conditions (Figure 1). We also assessed TMT labeling as an alternative to derivatization with propionic anhydride. This systematic approach allowed us to assess digestion efficiency, protein sequence coverage, labeling efficiency, and identification of common histone PTMs under rigorously controlled conditions. In addition to confirming recent reports of Arg-C Ultra's superior specificity, our analysis revealed that TMT labeling provides unique advantages for detecting negatively charged acylations through charge compensation at the peptide N-terminus. We further demonstrated that r-Chymotrypsin provides complementary sequence coverage for H2A variants and linker histones that are poorly represented by arginine-specific cleavage. As a proof-of-concept, we performed our streamlined dual-protease protocol, RIPUP (Rapid Identification of histone PTMs in Underivatized Peptides), on histones extracted from rat hippocampal sections to identify peptidoforms and PTM sites of biological interest in under 3 hours of sample preparation time.

Methods

Adult male Sprague-Dawley rats used in this study (Charles River Laboratories, Raleigh, NC) were kept in accordance with the ARRIVE guidelines and were approved by the Scripps Research Institute (TSRI) Animal Care and Use Committee (IACUC #09-0006), consistent with the National Institutes of Health Guide for the Care and Use of Laboratory Animals. The animals were housed in a temperature- and humidity-controlled room (12 h reverse light cycle) and provided with food and water *ad libitum*. The rats (n = 5, 446 ± 17.8 g) were anesthetized with isoflurane (3%), decapitated, and the brains were rapidly removed and placed into ice-cold high-sucrose cutting solution (206.0 mM sucrose, 2.5 mM KCl, 0.5 mM $CaCl_2$, 7.0 mM $MgCl_2$, 1.2 mM NaH_2PO_4, 26 mM $NaHCO_3$, 5.0 mM glucose, and 5 mM HEPES) gassed with 95% O_2 and 5% CO_2 [16,17]. A Vibrotome VS1000 (Leica Microsystems) was used to cut 300 µm coronal slices containing hippocampus (AP: -2.00 to -3.25 from bregma). The slices were transferred to cold, oxygenated (95% O_2 and 5% CO_2) artificial cerebrospinal fluid (130 mM NaCl, 3.5 mM KCl, 1.25 mM NaH_2PO_4, 1.5 mM $MgSO_4$, 2 mM $CaCl_2$, 24 mM $NaHCO_3$, and 10 mM glucose) and hippocampi were isolated and collected in 1.5 mL microcentrifuge tubes. Following isolation, hippocampi were immediately snap-frozen by placing the sample tubes into dry ice and transferred to cold storage at -80 °C until sample processing.

Histone extraction

Histones were extracted from HEK293T cells using an established protocol as described by Sidoli *et al* [7] (Figure 1). Briefly, frozen-thawed aliquots of HEK293T cells were pooled by transferring to a 50 mL falcon tube, and the tube topped with DPBS warmed to 37 °C. Cells were washed twice by centrifugation and the cell pellet was resuspended in chilled nuclear isolation buffer (NIB) [7] with DTT and protease inhibitors (Pierce EDTA-free protease inhibitor cocktail, ThermoScientific). Cells were washed once in NIB, lysed with NIB containing 0.2% NP-40 alternative, and homogenized by gentle pipetting. The mixture was incubated on ice for 10 min and centrifuged to pellet nuclei. The nuclei pellet was washed three times with NIB by centrifugation to remove traces of detergent, and the supernatant was discarded after the final wash. For rat hippocampal sections, frozen samples were thawed on ice, washed once with chilled NIB, transferred to a 2 mL dounce homogenizer, and homogenized/lysed with 10 – 15 strokes of the fine pestle. All other nuclei isolation steps were the same as described for nuclei extraction from HEK293T cells.

Acid extraction of histones from the nuclei pellets was performed by resuspending nuclei in 0.2 M H_2SO_4 and incubating at 4 °C for 2-3 h with gentle rotation. Insoluble material was removed by dual rounds of centrifugation, and trichloroacetic acid (TCA; 100%) was added to the supernatant to a final concentration of 33%, vortexed to mix, and incubated on ice overnight to precipitate histones. Pelleting and washing of precipitated histones with acetone/HCl and 100% acetone were performed as previously described [1]. The final histone pellets were resuspended in ddH_2O and centrifuged briefly to pellet insoluble material. The supernatant was transferred to a new tube and assessed for quality by SDS-PAGE and protein concentration by BCA assay (Pierce™ BCA Protein Assay, cat number 23227, Thermo Scientific™). For HEK293T samples, the sample was divided into aliquots of ~5 µg protein according to Tables 1 and 2, with four technical replicates in each condition, resulting in a total of 40 samples. For rat hippocampal sections, 2.5 µg of purified histones were used per protease (5 µg total per sample).

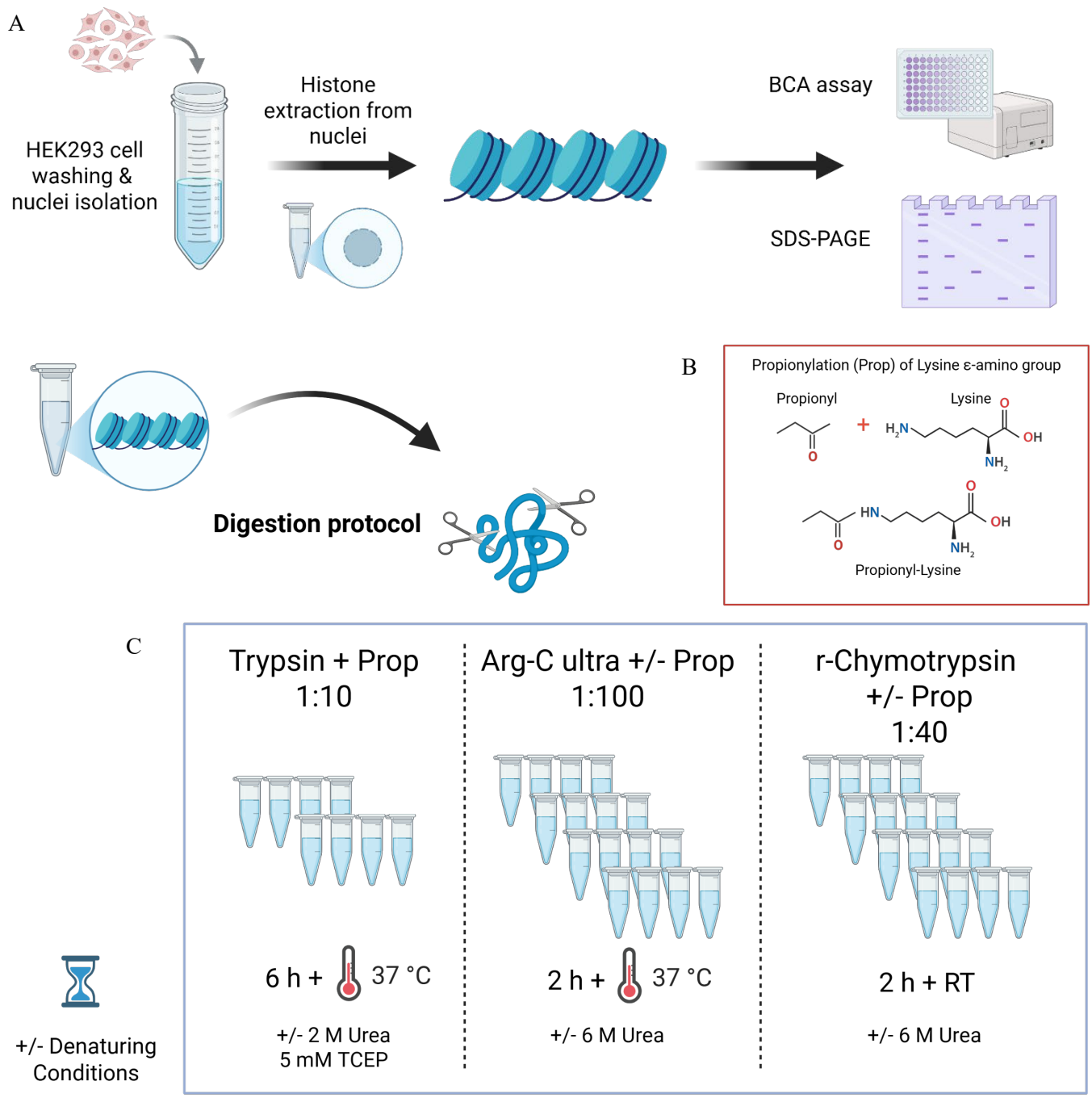

Figure 1. Experimental workflow for histone extraction and quality control from cell culture samples. HEK293T cells (A) were washed, homogenized, and processed for nuclei isolation, followed by acid extraction of histones from purified nuclei. Extracted histones from both sample types were quantified using bicinchoninic acid (BCA) protein assay and assessed for purity by SDS-PAGE to confirm successful extraction and appropriate histone band patterns before downstream proteomic analysis. Extracted histones were subjected to enzymatic digestion using three different protease conditions with or without chemical propionylation (Prop) and denaturing agent (2 or 6 M urea). (B) Addition of a propionyl group to lysine ε-amino groups, which neutralizes positive charges but prevents Trypsin cleavage at lysine residues, enabling retention of shorter peptides for higher sampling of histone PTMs. (C) Digestion conditions for systematic evaluation of Trypsin, Arg-C Ultra, and r-Chymotrypsin. Conventional Trypsin-based workflow with propionylation at 1:10 enzyme-to-substrate ratio, requiring 6 hours incubation at 37 °C. Samples were prepared with or without denaturing conditions. Arg-C Ultra digestion at 1:100 enzyme-to-substrate ratio with or without propionylation, requiring only 2 hours at 37 °C. Prototype recombinant chymotrypsin (r-Chymotrypsin) digestion at 1:40 enzyme-to-

substrate ratio with or without propionylation, performed at room temperature (RT) for 2 hours. All conditions were systematically evaluated for digestion efficiency, labeling completeness, PTM coverage, and generation of informative peptides suitable for quantitative PTM analysis by mass spectrometry.

Table 1: Protease digestion conditions for histones extracted from HEK293T cells.

Sample type	Protease	Denaturation	Derivatization (propionylation)	Digestion conditions: time (temperature)
HEK293	Trypsin (control) 1:10	+/-	+ (before and after digestion)	6 h (37 °C)
	Arg-C ultra 1:100	+/-	+/- (after digestion)	2 h (37 °C)
	r-Chymotrypsin 1:40	+/-	+/- (after digestion)	2 h (RT)

Table 2: Denaturing conditions for histones extracted from HEK293T cells.

Enzyme	Cleavage Specificity	Denaturant	Denaturant concentration
Arg-C Ultra	R; C-term	Urea	6 M (with 10 mM TCEP)
r-Chymotrypsin	Y, F, L, M; C-term	Urea	6 M (with 5 mM TCEP)
Trypsin	R, K (non-propionylated); C-term	Urea	2 M (with 5 mM TCEP)
Arg-C Ultra		None	(with 10 mM TCEP)
r-Chymotrypsin			(with 5 mM TCEP)
Trypsin			(with 5 mM TCEP)

SDS-PAGE

Aliquots of 5 µL extracted histones were mixed with 4x LDS sample buffer (NuPAGE™, Catalog number NP0007, Invitrogen™) and 10x sample reducing agent (NuPAGE™, Catalog number NP0009, Invitrogen™), to achieve a 1x final concentration in the sample. Samples were reduced for 10 min at 70 °C and 450 rpm in a Thermomixer (ThermoScientific). A volume equivalent to 2 µg total protein of purified histone H2A standard (Sigma-Aldrich, Cat number H9250, Sigma-Aldrich) was prepared in the same way. A 5 µL aliquot of protein ladder (BLUEstain™ 2 Protein ladder, 5-245 kDa, Cat Number: P008-500, Goldbio), samples, and H2A standard were separated by gel electrophoresis on a 4-12% Bis-Tris mini protein gel, 1.0–1.5 mm (NuPAGE™, Cat number: NP0321BOX, Invitrogen™) for 50 min at 150 V. The protein gel was placed into a clean gel tray and incubated with Acquastain gel stain (Bulldog Bio) to visualize protein bands. Gels were imaged on a gel imager with 5 s exposure (Azure biosystems c600).

MS sample preparation

We evaluated two different workflows against the established Trypsin with peptide N-terminal and K derivatization protocol: denaturing vs. non-denaturing and derivatized vs. non-derivatized for Arg-C Ultra (MS grade, Cat number: VA1831, Promega™) and r-Chymotrypsin (MS grade, Cat Number: CS3332042, Promega™; Table 1 and Figure 1). We also introduced TMT-labeling of Arg-C Ultra and r-Chymotrypsin digested peptides as an alternative to derivatization with propionic anhydride.

Protease digestion

Extracted histone samples were subjected to proteolytic digest with Arg-C Ultra or r-Chymotrypsin in 100 mM ammonium bicarbonate (AMBIC) under the conditions shown in Tables 1 and 2, according to the manufacturer's recommendations. The pH of all buffers were tested using pH strips (Cat Number: 13640521, Fisher Scientific) to ensure the pH was maintained at 8-8.5. Digestions with Arg-C Ultra (1:100) and r-Chymotrypsin (1:40 or 1:10) were performed in 10 µL reactions at 37 °C and RT, respectively, for 2 h in a thermal cycler (Biorad, MJ Mini). For histones extracted from rat hippocampi, we used Arg-C Ultra (1:10) and r-Chymotrypsin (1:10) in 20 µL reactions.

When labeling with TMT, HEK293T histones (5 µg) were digested in 100 mM TEAB pH 8.5, with Arg-C Ultra (1:100) or r-Chymotrypsin (1:10).

Derivatization (Propionylation)

Samples belonging to the Trypsin digestion groups were propionylated prior to digestion to prevent cleavage at the C-terminal of unmodified K residues. Samples were suspended in 50 mM AMBIC pH 8.0 to a final volume of 20 µL. The propionylation reagent was prepared as previously described [1] and all propionylation steps were performed in a fume hood. One batch of proprionylation reagent was used for up to 4 samples, and the propionylation was performed twice. Following the second round of propionylation, samples were dried in a vacuum centrifuge and stored at -80 °C until proteolytic digestion. Dried samples were resuspended in 10 µL digestion buffer containing Trypsin (Trypsin Gold, MS Grade, Promega, V5280) in 100 mM AMBIC pH 8.5. For the 'Trypsin + Urea' group, the digestion buffer also contained 2 M Urea and 5 mM TCEP (Table 2). Digestion reactions were incubated at 37 °C in a Thermomixer (Eppendorf) for 6 h. The reaction was stopped by freezing at -80 °C. The next day samples were thawed and dried in a vacuum concentrator. Two more rounds of propionylation were performed on Trypsin-digested samples and samples digested with Arg-C Ultra and r-Chymotrypsin (volumes adjusted with ddH_2O to final concentration 50 mM AMBIC) to label peptide N-termini and remaining K residues (Table 1). Finally, propionylated peptides were dried and resuspended in 10 µL 0.1% formic acid (FA) in de-ionized water.

Tandem Mass Tag (TMT) labeling

Histone peptides suspended in ddH_2O were mixed with TEAB to a final concentration of 100 mM, pH 8.0. Arg-C Ultra-generated peptides were labeled with TMT^{10}-126, and r-Chymotrypsin generated peptides were labeled with TMT^{10}-131 (cat no 90309, Thermo Scientific; monoisotopic mass = 229.162932) as per the manufacturer's instructions (peptide:TMT ratio 1:8, final concentration of anhydrous acetonitrile = 44%) for 1 h at RT in a 9 µL reaction. Free TMT was quenched by adding 1 µL of 5% hydroxylamine to the reaction and incubating for 15 min at RT. Labeled peptides were dried in a vacuum concentrator and resuspended in 0.1% FA in de-ionized water.

Peptide concentration was determined in samples digested with Trypsin (non-denaturing conditions) by colorimetric peptide assay (Pierce Colorimetric Peptide Assay Kit, Thermo Scientific). Peptide samples were diluted 1:100 with 0.1% FA, and 20 µL (~ 50 ng) aliquots were loaded onto Evotips (Evosep) following the manufacturer's instructions.

LC-MS/MS analysis

Mass spectrometry analysis was performed using a Thermofisher Scientific Fusion Lumos Tribrid Mass Spectrometer configured with an electrospray ionization (ESI) source and operated in positive ion mode. The instrument was interfaced with an Evosep One nanoLC system (Evosep). The mobile phase comprised Solvent A (H_2O with 0.1% FA) and Solvent B (ACN with 0.1% FA) (LC-MS grade, Fisher Scientific).

Reversed-phase HPLC separation was achieved using a custom-packed analytical capillary column (25 cm length, 150 nm internal diameter) containing Waters BEH C18 resin (1.7 µm particle size). Eluted peptides were introduced into the mass spectrometer via nanoelectrospray with a 2 kV spray voltage applied to the column inlet. Peptide fragmentation was performed using High-Energy Collisional Dissociation (HCD) in the Orbitrap. For non-TMT peptides, a fixed collision energy of 30% was applied, while TMT-labeled peptides were fragmented using a stepped normalized collision energy (NCE) of 30%, 40%, and 50% [18]. The analytical method employed a 15 spd LC gradient (88 minutes) at 220 nL/min.

DDA

Full MS scans were collected at 120K resolution in the Orbitrap over a scan range of 375 – 1500 *m/z* in profile mode. Default charge state was set to +2, cycle time was 3 s, and maximum injection time was 50 ms. Included charge states were +2 to +7, dynamic exclusion was set to 5 s, and precursor mass tolerance was set to 10 ppm. All precursors above the minimum intensity of $5e^4$ during the 3 s cycle time, or up to the AGC target of $4e^5$ ions, were selected for HCD MS/MS scans in the Orbitrap at 7.5K resolution and collected as centroided data. Maximum injection time for MS/MS scans was set to 100 ms, with an AGC target of $5e^4$. Isolation was performed in the quadrupole with an isolation window of 1.6 *m/z*.

Data analysis

Protein and PTM identification

MS raw files were processed in FragPipe (v24.0) following the recommended guidelines for the HiP-Frag workflow, with some modifications [15]. Data were searched against a restricted database containing extracted human or rat histone sequences, contaminants and decoys (*Homo sapiens*: 342 sequences, 171 decoys; *Rattus norvegicus*: 292 entries, 146 decoys; contaminants lists were derived from and curated by Cambridge Centre for Proteomics (CCP) cRAP). The enzyme cleavage parameters were adjusted for Arg-C Ultra and r-Chymotrypsin to cleave after R or FLYM, respectively. Up to 2 missed cleavages were allowed for Arg-C Ultra and Trypsin (set to cleave after R only) and up to 3 missed cleavages were allowed for r-Chymotrypsin. An additional Trypsin search was conducted using the default cleavage specificity (KR) and missed cleavages (5) as an additional assessment of the effects on peptide diversity resulting from incomplete propionylation of internal K residues. N-terminal propionylation was enabled as a static modification for all propionylated samples. For propionylated and non-propionylated samples, propionylation was set as a variable modification on K to account for endogenous propionylation in the case of the latter [19]. All default variable modifications

and mass offsets were enabled as per default pipeline settings, except methylation (+14.01565 Da) was added as a variable modification to non-propionylated samples (default setting +70.0419 Da, the combined mass of a propionyl group and methyl group), and the +70.0419 Da mass was retained as endogenous butyrylation. Propionylation on serine, threonine, and tyrosine was removed from the detailed mass offset list for non-propionylated samples. For TMT-labeled samples, the monoisotopic mass of the intact label (+229.162932 Da) was set as a static modification on peptide N-termini and as a variable modification on K, and all other PTM declarations were consistent with unlabeled samples. Finally, there were specific mass shifts considered for Gly-Gly (GG; +114.0429 Da) or Arg-Gly-Gly (RGG; +270.1441 Da) remnants corresponding to cleavage of ubiquitinylated K (Arg-C Ultra and r-Chymotrypsin cleaved ubiquitin, respectively. These fragments can also be labeled with propionyl or TMT at the free amine at the N-terminus, so +170.0691 Da (GG + Prop) and +343.2058 Da (GG + TMT) for Trypsin or Arg-C Ultra-digested samples, and +326.1703 Da (RGG + Prop) and +499.307 Da (RGG + TMT) for r-Chymotrypsin-digested samples were included. Label-free quantification (LFQ) and match-between-runs (MBR) were enabled for quantification. The propionyl and TMT masses were removed from peptidoforms during data analysis to enable direct qualitative comparison of identified peptidoforms between conditions.

Data processing and statistical methods

Data resulting from HiP-Frag output were imported into RStudio (RStudio 2025.09.2+, Build 418) and analyzed using custom R scripts. Reproducibility was assessed by calculating coefficients of variation (CV) from log2-transformed peptide intensities across technical replicates (n = 4 per condition for HEK293T samples; n = 5 for rat hippocampal samples). Digestion efficiency was evaluated by quantifying the proportion of peptides with 0, 1, or ≥2 missed cleavages. Labeling efficiency was calculated for both propionylation and TMT derivatization using two complementary metrics. For each peptide, lysine residues were classified based on modification status: labeled (bearing the expected derivatization mass: +56.026 Da for propionyl; +229.163 Da for TMT), free (unmodified), or biologically modified (e.g., acetylation, methylation). Biologically modified sites were excluded from calculations as they are not substrates for chemical derivatization. Site-based efficiency was calculated as labeled sites divided by the sum of labeled and free sites, expressed as a percentage (Efficiency (by site) = [labeled sites / (labeled sites + free sites)] × 100). Intensity-weighted efficiency was calculated by weighting each site count by peptide MS1 intensity, accounting for relative peptide abundance (Efficiency (by intensity) = [Σ(labeled sites × intensity) / (Σ(labeled sites × intensity) + Σ(free sites × intensity))] × 100). For TMT samples, both lysine residues and peptide N-termini were evaluated; for propionylation, only lysine residues were considered. Informative peptides were defined as those that were fully labeled, contained ≤1 missed cleavage, and were detected in ≥3 replicates. Histone protein sequence coverage was calculated as the percentage of theoretical amino acid sequence represented by identified peptides. PTM diversity was quantified by counting unique modification types at specific residue positions (e.g., H4 K8ac K12ac = 2 acetylations). For histones extracted from frozen-thawed rat hippocampal sections processed using the RIPUP protocol, peptidoforms were retained if detected in ≥2 replicates. Data are presented as means ± standard deviation or medians where appropriate.

Results

Protease and digestion conditions comparison

To assess potential improvements over the conventional Trypsin digestion with propionylation derivatization protocol, we systematically evaluated two alternative proteases, Arg-C Ultra and r-Chymotrypsin, under various experimental conditions including propionylation (Prop), urea denaturation, and TMT as an alternative to propionylation labeling. Our analysis focused on key performance metrics including total peptide identifications, digestion efficiency, sequence coverage, and the generation of informative peptides suitable for PTM identification and quantification. The reproducibility of protease activity and subsequent analyses via the developed pipeline were found to be robust, with median peptide CVs < 5% for all conditions (Figure 2A).

The three proteases tested generated peptides with distinct length distributions when considering complete cleavage (Figure 2B). Short/hydrophilic peptides generated by protease action are often lost during chromatographic separation resulting from poor solid-phase retention, explaining over-representation of longer peptides (median peptide length >15 amino acids) when treating non-propionylated substrates with proteases. Further denaturation of substrates by urea increases the length range of identified peptides generated by r-Chymotrypsin, whose protease activity is known to be sensitive to any remnant secondary structures [20]. In contrast, propionylation improves the hydrophobicity of short peptides, which reduces the median length of identified peptides in propionylated samples considerably, irrespective of urea denaturation. Trypsin and Arg-C Ultra showed similar cleavage specificity on propionylated histones, with a similar median peptide length of ~15 amino acid in both conditions that was unaffected by the presence of urea.

Arg-C Ultra digestion yielded substantially higher peptide identifications than the conventional 'Trypsin + Prop' approach (Figure 2C). Considering only the peptides with 0 missed cleavages, digestion with Arg-C Ultra resulted in the identification of 163 distinct histone peptides. Additional propionylation dramatically improved peptide identification to 254 distinct histone peptides, likely due to increased hydrophobicity, peptide retention and separation during LC. Notably, Arg-C Ultra demonstrated superior digestion efficiency with most identified peptides showing no missed cleavage (~84%, with and without propionylation, in absence of urea), whereas 'Trypsin + Prop' produced a more heterogeneous mixture containing peptides with one or more missed cleavages. The addition of urea generally increased the number of missed cleavages across all enzyme types, though this effect was minimal with Arg-C Ultra (~70% peptides without missed cleavage), and urea decreased the total number of peptides generated when the substrate was not propionylated. This could be attributed to the denaturing effect of urea being more pronounced on the protease activity than on the substrate that is already denatured by acid extraction.

r-Chymotrypsin followed similar trends, though fewer peptides were generated than Arg-C Ultra and higher missed cleavage rates were observed. r-Chymotrypsin performed similarly at the 1:10 and 1:40 enzyme-to-substrate ratios (49 and 45 peptides with no missed cleavages, respectively i.e., ~20-25% peptides). In the presence of urea, fewer peptides were generated, though fully cleaved peptides still formed ~21% of the total. However, in contrast to Arg-C Ultra, propionylation decreased the number of peptides generated with r-Chymotrypsin: only 7 fully cleaved peptides (~8% peptides) were identified. In contrast to Arg-C Ultra, urea boosted overall digestion and fully cleaved peptide numbers of propionylated histone peptides to 128 (~42% peptides), though substantially increasing missed cleavages.

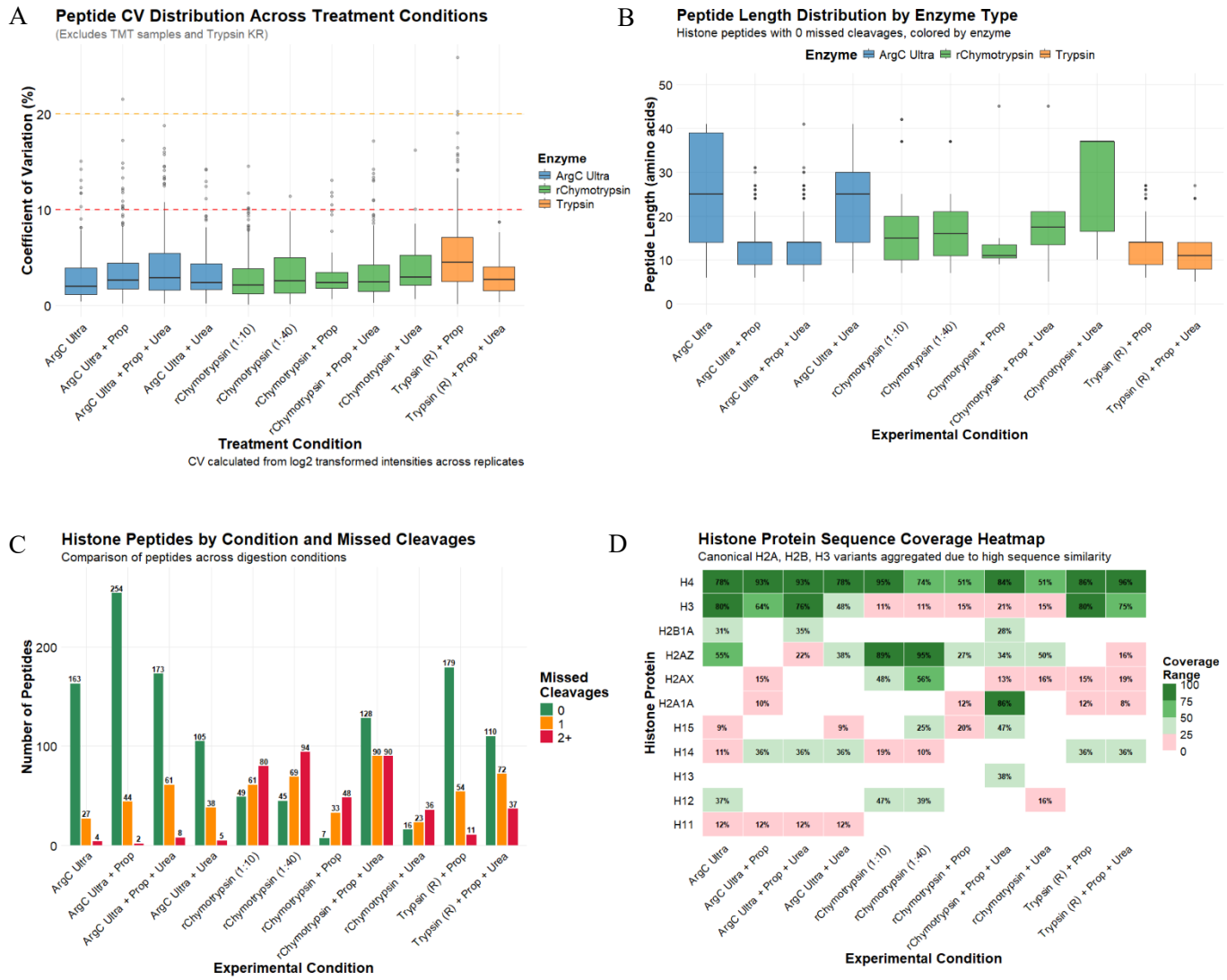

Figure 2. Comparative analysis of enzymatic digestion and propionylation strategies for histone post-translational modification detection in HEK293T cells (*n* = 4/condition). (A) Peptide coefficients of variation (CV) by enzyme type. All enzymes yield CVs < 10 %. (B) Peptide length distributions for peptides with 0 missed cleavages. Propionylation facilitates identification of shorter peptides. (C) Number of histone peptides identified across experimental conditions, stratified by missed cleavages (0, 1, or 2+). Arg-C Ultra consistently yields the highest peptide counts with minimal missed cleavages. (D) Sequence coverage heatmap for canonical histone proteins across experimental conditions. H3 variants (H3.1, H3.2, H3.3) are aggregated due to high sequence similarity. Coverage values represent percentage of protein sequence covered by identified peptides.

Histone protein sequence coverage

We assessed the impact of different enzymatic digestion strategies on histone protein sequence coverage, with histone sub-variants aggregated due to high sequence similarity (Figure 2D). Core histone H4 exhibited the highest sequence coverage across all conditions, with ~75-95% coverage consistently achieved across most conditions. H3 coverage was highest (80%) with Arg-C Ultra and 'Trypsin + Prop', however sequence coverage provided by r-Chymotrypsin was

low (~10-20%). r-Chymotrypsin provided high sequence coverage for H2A variants, H2A.Z (95%, when used at 1:40) and H2A1A (86% with 'r-Chymotrypsin + Prop') compared to minimal or no sequence coverage with Arg-C Ultra and Trypsin. Linker histone H1 variants (H1.1, H1.2, H1.3, H1.4, H1.5) exhibited variable coverage across enzyme types, with r-Chymotrypsin outperforming Arg-C Ultra and Trypsin in most cases except H1.4 where Arg-C Ultra and Trypsin perform better. H1.2 and H1.5 were covered up to 47% with r-Chymotrypsin. The complementary coverage patterns observed across the three enzymatic approaches underscores the value of employing orthogonal digestion strategies to maximize histone proteome characterization and PTM site accessibility.

Chemical Rationale for TMT Labeling

In this study, we used TMT labels as derivatization agents because of their hydrophobicity and high labeling efficiency, independent of their conventional use as multiplexed isobaric labels for quantitating conditional changes in protein abundance [12]. TMT and propionyl derivatization both target primary amines (N-termini and K ε-amines) via NHS ester and anhydride chemistry, respectively, forming stable amide bonds [2]. However, the structural differences between these modifications impact peptide behavior during LC-MS/MS. Propionylation introduces a small aliphatic acyl group (+56.026 Da) that increases peptide hydrophobicity due to its purely hydrocarbon character (Figure 3A and 3B). This results in extended retention times on reversed-phase columns and can still result in co-elution of multiply modified histone peptides, particularly those derived from the K-rich N-terminal tails of histones H3 and H4. In contrast, TMT labels (~229.1629 Da for TMT^{10}) have multiple polar functional groups, including carbonyl oxygens and a tertiary amine within the reporter region. This structural composition confers moderate rather than high hydrophobicity, resulting in earlier retention times than propionylated counterparts. Propionylated histone peptides, particularly those with multiple modified K residues, can elute late in the reversed-phase gradient where chromatographic resolution may be suboptimal.

Importantly, the tertiary amine within the TMT reporter region shows high proton affinity. According to the mobile proton model of peptide fragmentation [21], protons migrate along the peptide backbone during collision-induced dissociation and direct bond cleavage. In conventional tryptic and Arg-C-like peptides, mobile protons preferentially localize toward the C-terminus, favoring *y*-ion formation (Figure 3C) [22]. The TMT tertiary amine sequesters a mobile proton at the N-terminal region of the peptide, shifting fragmentation dynamics to enhance *b*-ion series generation. This effect was particularly pronounced when using stepped collision energies of 30, 40, and 50 (normalized), which provided sufficient energy to fragment the peptide backbone while the TMT moiety retained the sequestered proton.

The enhanced *b*-ion coverage has direct implications for histone PTM analysis, where confident localization of PTMs requires the presence of flanking fragment ions on both sides of the modification site (Figure 3D). For histones, where multiple modifications often occur in close proximity on the same peptide, the enhancement of *b*-ions provided by TMT improves site localization confidence and peptidoform discrimination (Supplementary Table S3).

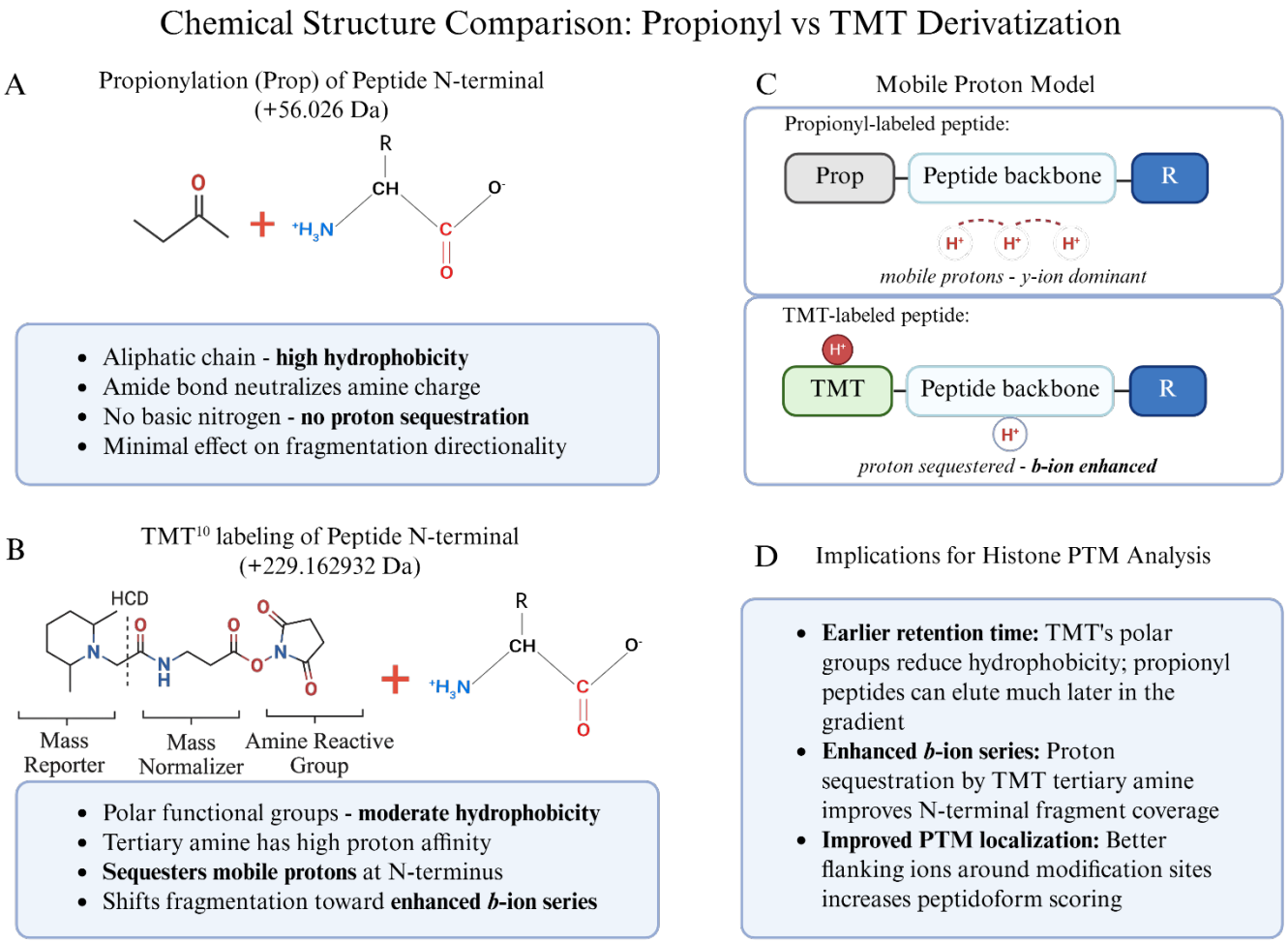

Figure 3: Chemical and structural comparison of propionylation and TMT derivatization strategies for histone peptide analysis. (A) Propionylation of peptide N-terminal amines using propionic anhydride (+56.026 Da). The propionyl group is a small aliphatic chain that increases hydrophobicity and neutralizes the amine charge but contains no basic nitrogen capable of proton sequestration. (B) TMT^{10} labeling of peptide N-terminal amines (+229.1629 Da). The TMT label comprises three functional regions: a mass reporter containing a tertiary amine with high proton affinity, a mass normalizer incorporating heavy isotopes (e.g., ^{13}C, ^{15}N), and an amine-reactive NHS ester group. The tertiary amine within the reporter region can sequester mobile protons during collision-induced dissociation. (C) Mobile proton model illustrating differential fragmentation behavior. In propionyl-labeled peptides, protons remain mobile along the peptide backbone, favoring *y*-ion formation. In TMT-labeled peptides, the tertiary amine sequesters a proton at the N-terminus, shifting fragmentation dynamics toward enhanced *b*-ion series generation. (D) Summary of implications for histone PTM analysis. Image of TMT structure in (B) was adapted from Thermo Scientific Pub. No. MAN0016969, Rev B.0, Pub. Part No. 2162457.5 (Figure 2). Created in https://BioRender.com.

Initial TMT assessment

Current methods of histone PTM analysis rely on efficient labeling/chemical propionylation of K and peptide N-termini to ensure robust PTM identification, quantification, and reliable comparison between two or more groups [8,10,23]. However, it is well-documented that propionylation can be highly variable, with both under- and over-propionylation

affecting downstream quantification [10]. This was apparent when we included C-terminal of K as a potential site of Trypsin cleavage in the 'Trypsin + Prop' condition, where it is assumed that all lysines are propionylated and hence unavailable for Trypsin cleavage. Inclusion of K in cleavage specificity increased the number of identified peptides by ~2.2 fold (~2.4 fold considering peptides with 0 missed cleavages) compared to when only C-terminal of R Trypsin cleavage is included, suggesting that many lysines are not propionylated and therefore available for cleavage (Figure S1A). For this reason and those described in the previous section, we performed an assessment of TMT as an alternative labeling strategy to propionylation. Although the use of TMT for histone PTM analysis has been suggested elsewhere [24] and demonstrated for histone H3 middle-down proteomics analysis [25] , as well as for quantification of DNA damage-associated changes to histones following chromatin cross-linking in yeast [26], there has been no direct comparison of TMT to propionylation or other chemical derivatizing agents such as TMA [9], phenyl isocyanate (PIC) [24], or d^6-acetic anhydride + PIC [23] for labeling histone-peptides. We compared the Arg-C Ultra and r-Chymotrypsin (1:10) generated peptides labeled with TMT to the established method of 'Trypsin + Prop', as these alternatives facilitate rapid sample processing with ≤ 2 h digestion times and only one round of labeling post-digestion. We first assessed the key metrics described in Figure 2 against 'Trypsin + Prop', labeling efficiency by site count and intensity, and then determined the number of informative peptides that could be used for quantification i.e., fully labeled peptides with ≤ 1 missed cleavage and no artifacts (e.g., Methionine oxidation).

The median peptide CVs of TMT-labeled Arg-C Ultra and r-Chymotrypsin peptides were lower than 'Trypsin + Prop' peptides (Figure S1A). Median lengths of fully cleaved and TMT-labeled peptides generated by Arg-C Ultra and r-Chymotrypsin were similar to peptides from 'Trypsin + Prop' (~10-15 amino acids; Figure S1B). TMT-labeling yielded ~1.2-fold more fully cleaved peptides with Arg-C Ultra than the established 'Trypsin + Prop' approach (217 vs 179; Figure S1C); 'Arg-C Ultra + Prop' yielded 1.17-fold more completely-cleaved peptides than TMT-labeling (254 vs 217; Figure 2C and Supplementary Figure S2C); TMT-labeling yielded >15-fold more completely-cleaved peptides than propionylation when treated with r-Chymotrypsin (121 vs 7). Except for H4, histone sequence coverage deteriorated with Arg-C Ultra upon TMT-labeling (e.g., H3 decreased from 80% to 59%), while histone sequence coverage remained similar or improved when r-Chymotrypsin peptides were TMT-labeled, except H2A.X (48% to 0%; Figure S1D). Artifact rates such as methionine oxidation and dehydration on S/E/T/Q were 2% and 4.5%, respectively, for 'Trypsin + Prop'. This dehydration decreased to 0.6% and oxidation increased to 7.5% when Arg-C Ultra peptides were labeled with TMT, while both artifacts increased to 15.4% and 12.9%, respectively, in TMT-labeled peptides from r-Chymotrypsin digest (Figure S1E).

Labeling efficiency of propionic anhydride vs TMT

Trypsin cleavage at non-propionylated K resulted in the loss of ~58% of peptides (considering fully cleaved peptides) with 'Trypsin + Prop', which also prohibits the direct assessment of propionylation efficiency for Trypsin-digested samples (Figure S1F). However, we could directly assess propionylation efficiency for Arg-C Ultra and r-Chymotrypsin digests, where only one round of propionylation was performed post-digestion (Figure 4A). Considering only internal K as potential sites of propionylation (all peptide N-termini were considered propionylated, hence a static/fixed modification), propionylation efficiency calculated by site count (29-61%) was lower overall compared to estimation by intensity (33-71%). Efficiency of TMT-labeling was ~92% by site count and ~99% by intensity for peptides from Arg-C Ultra digest, and ~91% by site count and ~99% by intensity for peptides from r-Chymotrypsin digest.

Histone peptides that are reproducibly generated and identified with minimal variability are the best candidates for precise quantification and highly confident comparative analysis, which we termed informative histone peptides (IHP). We defined these as peptides with ≤ 1 missed cleavage, identified in 3 out of 4 replicates, and lacking common artifacts like methionine oxidation or dehydration (Figure 4B). The effect of labeling and its efficiency was significant on IHP, with unlabeled samples outperforming propionylated samples overall when considering the proportion of IHP among total identified peptides. Although labeling (TMT and propionylation) and the presence of urea generally increased the total number of identified peptides, they slightly decreased the proportion of IHP. As mentioned above, since we substantially underestimate the total peptides in 'Trypsin + Prop' samples due to partial propionylation of K resulting in Trypsin-cleavage at these unlabeled K residues, we substantially overestimate the proportion of IHP (87-90%) in 'Trypsin + Prop' conditions. Arg-C Ultra digests provide a high proportion of IHP (~80%) and r-Chymotrypsin digests yield ~40-50% IHP, which decreases to ~30-35% in the presence of urea or propionylation. TMT-labeling improved the number of IHP for both Arg-C Ultra and r-Chymotrypsin digestions (141 vs 170 and 100 vs 181, respectively), which was similar to IHP from 'Trypsin + Prop' condition (185) and 'Arg-C Ultra + Prop' (178).

To further explore the impact of suboptimal labeling on the number of IHP, we compared our search results from Trypsin with cleavage specificity set to R (for fully labeled K residues) to a separate search with cleavage specificity set to KR (for partially/unlabeled K residues; Supplementary Figure S1F). The number of fully labeled and properly cleaved peptides in 'Trypsin + Prop' (R) (179) constitutes ~33% of the total number of peptides obtained from this method (sum of all peptides from 'Trypsin + Prop' (KR); Supplementary Figure S1F).

Histone PTM identification

Histone PTM identificationArg-C Ultra and r-Chymotrypsin digestion achieved high PTM coverage, detecting up to ~120 unique modifications and over 15 distinct PTM types, including acetylation, methylation (mono-, di-, and tri-methyl states), ubiquitination (GG and RGG depending on digestion strategy), and acylations such as crotonylation, lactylation, succinylation, and malonylation (Figure 5). Arg-C Ultra resulted in high PTM numbers under most conditions, while 'r-Chymotrypsin + Prop + Urea' outperformed all other r-Chymotrypsin conditions substantially. Coverage of the most prevalent modifications (acetylation, methylation, and phosphorylation) was achieved across all conditions. Endogenous propionylation and butyrylation were identified in unpropionylated Arg-C Ultra and r-Chymotrypsin digested peptides, which cannot be distinguished from peptides labeled with propionyl +/- mono-methylation when propionic anhydride is used as a derivatizing agent. TMT-labeled peptides from Arg-C Ultra and r-Chymotrypsin digestion achieved comparable PTM numbers to conventional 'Trypsin + Prop' methods (~120 PTMs) and enhanced identification of specific modification-types, including pronounced enrichment of negatively charged acylation marks such as succinylation and glutarylation (Figure 5B). The TMT-labeling approach detected a greater diversity of PTM classes than propionylation while offering superior labeling efficiency. Propionylation enabled identification of glyceroyl sites across all three enzymes, minimally detected in TMT-labeled or unlabeled samples, whereas Arg-C Ultra +/- urea increased identification of ubiquitination remnants. As amine-reactive labels modify the N-terminal amino acid of the GG remnant, charge neutralization occurs during propionylation; the overall charge state of a propionylated vs. unpropionylated GG-containing peptide would be ~+1 vs. ~+3, respectively. Arg-C Ultra samples without propionylation are therefore more likely to be selected for fragmentation (≥+2 charge) and exhibit increased ionization efficiency for PTMs that suffer from charge neutralization during propionylation.

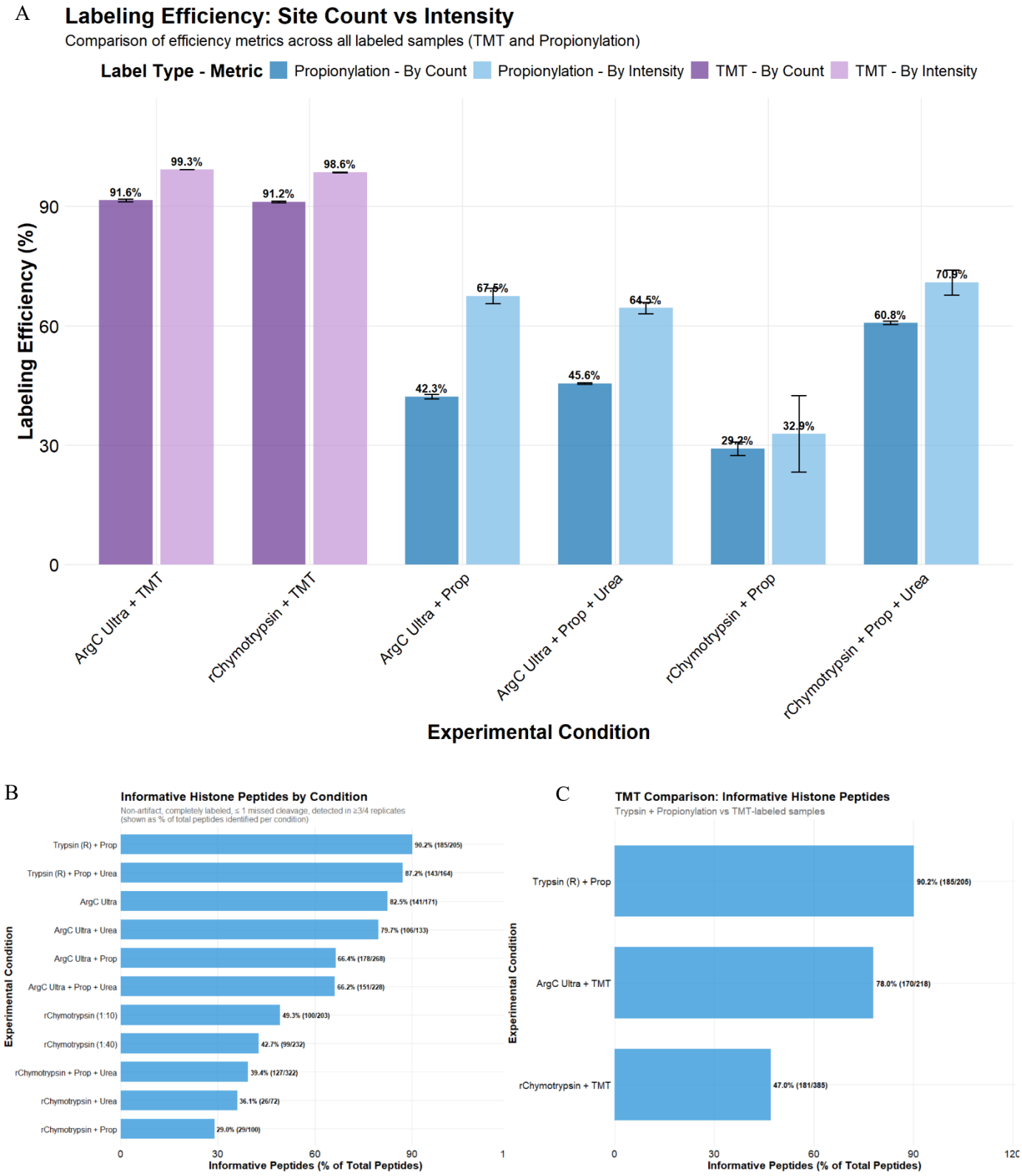

Figure 4. Comparison of internal lysine (K) labeling efficiency and informative peptide coverage across enzyme digestion strategies for histone PTM analysis. (A) Labeling efficiency metrics comparing propionylation and TMT-labeling approaches across all experimental conditions. Efficiency was calculated using two methods: by site count (darker bars) showing the percentage of sites that were successfully labeled out of all theoretically available sites for labeling, and by intensity (lighter bars) representing the sum of labeled peptide intensities divided by total peptide

intensity. TMT-labeling efficiency by intensity was >98% in Arg-C Ultra and r-Chymotrypsin (1:10) digested samples, compared to propionylation efficiency by intensity of ~68% in Arg-C Ultra and ~33% in r-Chymotrypsin. Error bars represent standard deviation across $n = 4$ digestion replicates. (B) Percentage of IHP identified across different enzyme digestion conditions where IHP are defined as peptides containing completely labeled N-termini and lysine residues. Searching the Trypsin-digested samples with R cleavage specificity overestimates labeling efficiency, as any unlabeled K residues would result in cleavage at the lysine C-terminus. These peptides are not included in the search results, except in the case of a missed cleavage event. This is evident in Figure 4B, where 'Trypsin + Prop' resulted in the highest IHP (~90%), with unlabeled Arg-C Ultra the second highest (~83%). (C) TMT-labeling improved the number of IHP generated by Arg-C Ultra (170 vs 141) and r-Chymotrypsin (181 vs 100), which was comparable to 'Trypsin + Prop' (185). Numbers in parentheses indicate IHP out of total peptides identified.

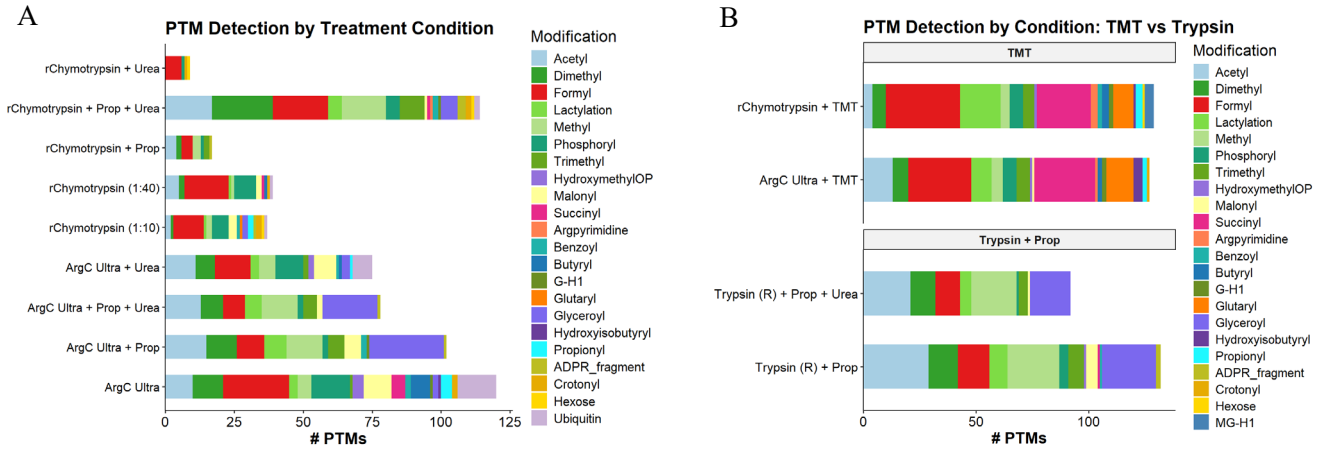

Figure 5. Diversity and abundance of histone post-translational modifications detected across enzyme digestion and chemical labeling strategies. (A) Total number and distribution of PTM types identified across different experimental conditions, including Arg-C Ultra, Trypsin, and r-Chymotrypsin digestion combined with propionylation (Prop), urea denaturation (Urea), or both (Prop + Urea). For r-Chymotrypsin, enzyme-to-substrate ratios of 1:10 and 1:40 were also tested without chemical derivatization. Each stacked bar represents the cumulative count of unique PTM sites detected, colored by modification type. (B) Comparison of identified PTMs between TMT-labeled peptides from Arg-C Ultra and r-Chymotrypsin and propionylated tryptic peptides. PTMs detected include common modifications (acetylation, mono-/di-/tri-methylation, formylation, phosphorylation, and ubiquitinylation) and less abundant modifications (lactylation, succinylation, malonylation, benzoylation, butyrylation, propionylation, glyceroylation, glutarylation, hydroxyisobutyrylation, hydroxymethyl-OP, argpyrimidine, AGEs including G-H1 and MG-H1, crotonylation, hexose modifications, and ADPR fragments). Ubiquitin remnants are identified in unlabeled Arg-C Ultra digests; propionylation identifies glyceroylation sites not detected in labeled samples. TMT labeling improves identification of succinylated and glutarylated peptides. Endogenous propionylation and butyrylation are discernible in non-propionylated Arg-C Ultra and r-Chymotrypsin peptides.

Enhanced identification of histone succinylation and glutarylation with TMT

Lysine succinylation and glutarylation are acidic acyl modifications that reverse the charge of modified residues from +1 to −1, destabilizing nucleosome structure and promoting chromatin accessibility [27,28]. Both modifications are enriched at promoters of active genes, regulated by acetyltransferases (KAT2A, p300/CBP) and sirtuins (SIRT5, SIRT7), and linked to metabolic state through their acyl-CoA donors [29–31]. Dysregulation of these modifications has been implicated in cancer, protein-protein and DNA-protein interactions, and defective DNA repair [14], yet their comprehensive profiling has been limited by suppressed ionization of acidic peptides in MS-based workflows. A striking and serendipitous finding from our evaluation was the dramatically enhanced identification of succinyl-lysine and glutaryl-lysine sites in TMT-labeled peptides (Figure 5B). While our current work and the recent study by Ryzhaya et al.[9] demonstrate that chemical derivatization at the peptide level improves histone PTM analysis, our data reveal that TMT provides unique advantages for identifying acidic acylations other than improved chromatographic retention alone.

Succinylation as a histone PTM is thought to occur less frequently than acetylation and methylation [13,27], though a recent study found that an increase in global histone succinylation is associated with longevity [32]. In the current study, succinylation was often identified on first or second position K residues, adjacent K residues, or near the peptide C-terminus, which are challenging regions for confident PTM localization. For r-Chymotrypsin peptides labeled with TMT, succinylation sites were identified in H1.4 (9 sites), H2B (6 sites), H4 (4 sites), H2A variants (3 sites), and H3 (2 sites), including regions not covered by Arg-C Ultra or 'Trypsin + Prop' approaches (Supplementary Figures S3 and S4).

The enhanced detection of succinyl-K with TMT is explained by the charge compensation provided by the tertiary amine within the TMT reporter region. Succinylation introduces a carboxylic acid moiety that impairs positive-mode ESI via charge state reduction. While propionylation increases peptide hydrophobicity, it neutralizes the charge of K residues and peptide N-termini. The TMT tertiary amine instead provides a compensating protonation site, rescuing ionization of succinylated peptides and increasing *b*-ion series flanking PTM sites (Figure 3, Supplementary Figures S3 and S4). This effect also extended to glutarylation (114.031694 Da) [33,34]. Others have studied these negatively charged modifications using synthesized succinyl-K and glutaryl-K thioester derivatives in recombinant histone proteins [14]. TMT-labeling thus offers a practical alternative for biological samples. In summary, the improvement in identification of succinylation (50 sites) and glutarylation (27 sites) with TMT-derivatization is attributable to improved ionization/fragmentation efficiency and PTM-site scoring, suggesting that succinylation of histone K residues may be more abundant than previously thought and revealing a PTM signature in HEK293T cells largely undetected by other methods and above what has been reported using MS-based methods [13,27,32].

Systematic Evaluation of Protease and Labeling Strategies: Advantages of a Multi-Protease Workflow

Our systematic comparison of proteases and labeling conditions across 40 samples builds upon recent reports of individual protease performance. While Ryzhaya et al. [9] demonstrated that Arg-C Ultra simplifies histone preparation and that TMA derivatization enhances separation of positional isomers, our comprehensive evaluation reveals additional complexity in method selection and highlights the value of complementary multi-protease strategies.

First, different proteases and labeling strategies are necessary to optimally sequence various histones and map different PTM classes. Arg-C Ultra excels at generating properly cleaved peptides with minimal missed cleavages (>99%

specificity for properly cleaved peptides in TMT-labeled samples), confirming recent reports of its improved performance over conventional Arg-C. However, r-Chymotrypsin provides critical orthogonal coverage for regions poorly represented by arginine-specific cleavage: specifically, 95% sequence coverage of H4, 80% of H2A.Z, and 36% of H2A1A, compared to minimal or no detection with Arg-C Ultra and 'Trypsin + Prop' (Figure S1D). This complementary coverage is essential for linker histone H1 variant characterization, which showed 28–47% coverage with r-Chymotrypsin compared to near-zero with other strategies.

Second, TMT and propionylation-based derivatization have distinct strengths beyond labeling efficiency. TMT's single-step labeling reduces workflow complexity and improves reproducibility, and its tertiary amine provides charge compensation rescuing ionization of negatively charged acylations, yielding 50 succinylation and 27 glutarylation sites, a dramatic increase over propionylation-based approaches. This suggests acidic histone acylations have been systematically underestimated with conventional methods, constituting what we term the 'dark epigenome'.

Third, our data supports a decision framework for method selection. For rapid screening where acidic acylations are of interest, RIPUP using Arg-C Ultra and TMT provides high labeling efficiency, excellent PTM coverage, and enhanced succinylation/glutarylation detection within ~3 hours. When comprehensive coverage of H2A variants and linker histones is required, r-Chymotrypsin digestion should be added. For positional isomer quantification, TMA-based workflows described by Ryzhaya et al. represent a viable alternative. Both substantially reduce preparation time compared to 'Trypsin + Prop' (~48-72 hours), with RIPUP offering the additional advantage of TMT multiplexing for comparative studies.

Finally, short hydrophilic peptides (<11 amino acids, ≥2 lysines) benefited substantially from chemical derivatization, with 170-177 IHP identified in TMT-labeled and propionylated conditions vs. 101-120 in unlabeled samples, while longer peptides (>15 amino acids) were better detected without derivatization. This underscores the value of a multi-protease, multi-condition strategy for comprehensive histone PTM coverage.

RIPUP of hippocampal sections

As a proof-of-principle experiment, we extracted histones from rat hippocampal sections and performed RIPUP using separate Arg-C Ultra and r-Chymotrypsin digestions. Total sample preparation time was ~3 h; we identified 212 and 189 peptides with ≤1 missed cleavage with Arg-C Ultra (1:10) and r-Chymotrypsin (1:10), respectively (Supplementary Figure S5A), with median CVs of ~7% for both (Supplementary Figure S5B). Combined, both enzymes detected 231 unique PTM sites, including all major PTM classes: acetylation, mono-, di-, and tri-methylation, phosphorylation, and ubiquitination (Figure 6A and B). Less common modifications were also detected, including endogenous propionylation and butyrylation, which are erroneously assigned as unmodified (prop) or mono-methylated (bu) when derivatized with propionic anhydride.

Analysis of selected core and variant histone sequences confirmed that highly modified N-terminal tails of H3 and H4 and ubiquitination sites K118/K119 on H2A were captured (Figure 6C). N-terminal acetylation and R3 mono- and di-methylation on H4, implicated in transcriptional regulation via PTM crosstalk [35–37], were identified, along with multiple peptidoforms of the H3 aa 9-17 and H4 aa 4-17 peptides enabling detection of combinatorial acetylation patterns with implications for chromatin structure and disease [6,38–40]. The critical H3 region (aa 27-40) and K79 mono- and di-methylation were detected in Arg-C Ultra-digested samples; methylation of H3 K27, K36, and K37 functions as

transcriptional activators or repressors via Polycomb silencing [41–43] and is crucial for interpreting gene expression anomalies in cancer [44].

RIPUP detected extensive PTM diversity on linker histone H1 variants. H1.4 contained 16 unique modification sites spanning residues 75-102, including succinylation at K75 and K90, crotonylation at K81, lactylation at K97, and arginine mono- and di-methylation at R79. H1.5 showed succinylation (K74) and crotonylation (K74, K80), while H1.9 displayed a complex modification profile at K96 (me3, pr, cr, bu) and K106 (me2, me3, cr, la, bu), plus ubiquitination (RGG remnant) at K97 by r-Chymotrypsin.

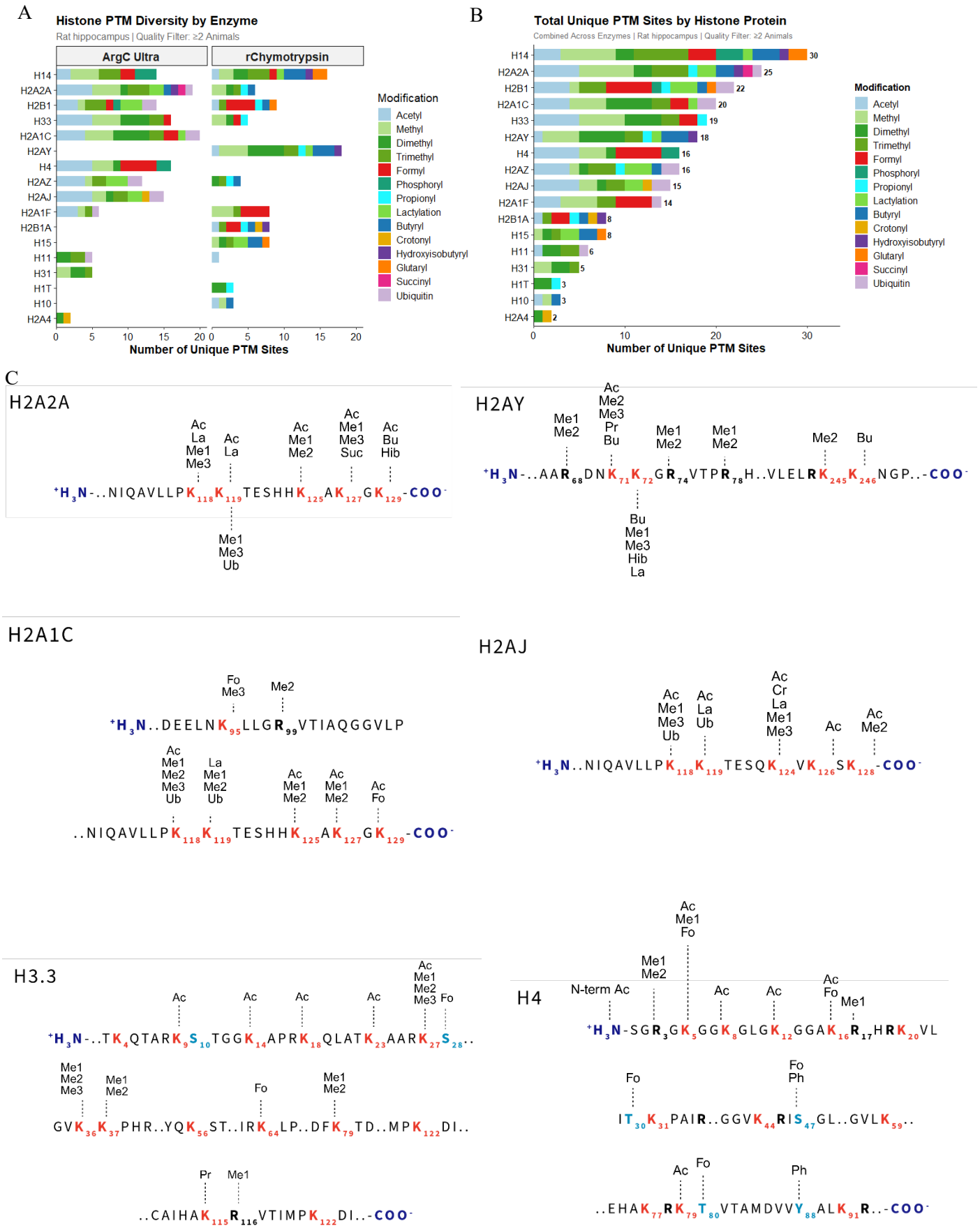

Figure 6. Comprehensive histone post-translational modification landscape in rat hippocampus. (A) Histone PTM diversity detected per enzyme strategy in ≥2 animals. Stacked bars show unique PTM sites per histone using Arg-C Ultra (left) or r-Chymotrypsin (right), colored by modification type. (B) Total unique PTM sites per histone combining both enzymes; H1.4 and H2A2A showed the greatest diversity (30 and 25 unique sites, respectively). (C) Site-specific

PTM maps for selected histone variants showing detected modification sites with K, R, S, and T residues highlighted. Subscript numbers indicate canonical residue positions. Abbreviations: Ac, acetylation; Me1/Me2/Me3, mono-/di-/trimethylation; Fo, formylation; Ph, phosphorylation; Ub, ubiquitination; La, lactylation; Bu, butyrylation; Cr, crotonylation; Hib, 2-hydroxyisobutyrylation; Pr, propionylation; Suc, succinylation; N-term, N-terminal modification. Data represent combined analysis from male rat hippocampi (n = 5). Figure 6C created in https://BioRender.com.

Core histone macro-H2A.1 exhibited arginine methylation at R69, R75, and R79, along with lysine modifications at K72 (ac, me2, me3, pr, bu) and K73 (me1, me3, cr, la, bu). H2B K59 emerged as a highly modified site, with seven distinct modification types at this single residue: acetylation, butyrylation, propionylation, lactylation, trimethylation, 2-hydroxyisobutyrylation, and ubiquitination (RGG remnant). Glutarylation was also detected on H2A K119, demonstrating the benefit of retained positive charge on underivatized peptide N-termini for detecting negatively charged PTMs.

Formylation of K, S, T, and Y residues was a prominent feature in both HEK293T and rat hippocampal histones, an observation also made by authors of the HiP-Frag workflow across multiple cell lines [15]. Although formylation can arise as a sample preparation artifact [45], this was not a feature of our workflow, and others have shown it to be an abundant and biologically important histone PTM on K [46–48], pointing to it as an epigenetic mark warranting attention in future studies.

Discussion

Computational Stringency Enables Large-Scale PTM Discovery: Positioning RIPUP Within Recent Advances

Recent work by Vai et al. (2025) addressed the challenge of PTM confirmation at scale by developing HiP-Frag, integrating mass offset, open, and closed search strategies for confident novel PTM identification through rigorous computational filtering rather than comprehensive synthetic validation [15]. Using this approach, they identified 60 previously unreported marks on core histones and 13 on linker histones across nine cancer cell lines and breast cancer tissue.

Our study extends this framework by applying HiP-Frag principles to a systematic comparison of protease and labeling strategies. Specifically, we demonstrate that TMT vs. propionylation dramatically influences which PTM classes are detected: propionylation neutralizes positive charges on K residues without providing charge compensation for negatively charged modifications, resulting in poor ESI efficiency, whereas TMT's tertiary amine rescues ionization of acidic acylations. This mechanistic explanation accounts for why succinylation and glutarylation may have been underreported with conventional workflows.

Importantly, TMT and propionylation workflows reveal complementary rather than competing PTM landscapes. Researchers interested in acidic acylations should consider TMT-based workflows, while those focused on positional isomer separation may benefit from TMA-based approaches [9]. The orthogonal nature of these methods underscores the value of multi-strategy approaches for comprehensive PTM characterization.

Application of RIPUP to rat hippocampal tissue confirms that computationally driven PTM discovery extends to complex biological samples, consistent with Vai et al.'s analysis of breast cancer tissues [15]. Detection of 231 unique PTM sites within a 3-hour workflow, including biologically critical marks such as H4 K5/K8/K12/K16 acetylation, H3

K27/K36/K37 methylation, and extensive linker histone modifications, validates RIPUP for time-sensitive biological discovery.

We applied 1% FDR at PSM and peptide levels, minimum detection in ≥3 digestion replicates (HEK293T) or ≥2 biological replicates (rat hippocampi), and CV filtering to ensure high-confidence assignments. The pragmatic validation approach used by Vai et al., which used targeted synthetic validation for ambiguous cases rather than comprehensive validation of all discoveries, is one we similarly adopt, and future studies could prioritize synthetic validation of the most abundant or biologically relevant succinylation and glutarylation sites identified here.

RIPUP: A Rapid Multi-Protease Workflow for Comprehensive Histone PTM Analysis

RIPUP introduces a strategic multi-protease approach that maximizes sequence coverage while minimizing sample preparation time. By combining Arg-C Ultra and r-Chymotrypsin, RIPUP provides access to distinct regions of the histone proteome: Arg-C Ultra efficiently covers N-terminal tails and generates quantitative information for abundant PTM sites, while r-Chymotrypsin captures H2A variants, linker histone H1 variants, and aromatic-rich regions poorly represented by arginine-specific cleavage.

Using the HiP-Frag framework, we identified 50 succinylation and 27 glutarylation sites in HEK293T cells, representing a substantial expansion of the known histone acylation landscape and suggesting these acidic acylations may have been systematically under-detected with conventional propionylation-based workflows. Application to rat hippocampal tissue demonstrated practical utility, identifying 231 unique PTM sites across both enzymes within 3 hours, including all major PTM classes, biologically critical sites on H3, H4, and H2A, and extensive linker histone H1.4 coverage that would have been largely missed using Arg-C Ultra or Trypsin alone.

The rapid turnaround is particularly advantageous for drug discovery targeting epigenetic modifiers or clinical contexts requiring rapid molecular profiling (e.g., intraoperative tumor assessment), where same-day assessment of histone PTM landscapes is operationally valuable. Additionally, RIPUP's dual-protease strategy provides built-in orthogonal validation: PTMs detected by both enzymes where coverage overlaps increase confidence in site assignment, while protease-specific detections expand the accessible PTM landscape [49–51].

Limitations

We acknowledge that systematic comparisons were performed in a single cell line (HEK293T), and performance may vary with different sample types or extraction protocols, though broader applicability is demonstrated through hippocampal tissue analysis. Validation of the succinylation/glutarylation enhancement across additional cell types or primary tissues would strengthen these findings. Despite our dual protease strategy, sequence coverage gaps persist, particularly within globular domains. The reported PTM landscape reflects only regions accessible to the enzymes studied, though the RIPUP protocol is compatible with alternative digestion strategies to improve coverage [49–51].

PTM identification is constrained by the variable modification search space defined in the HiP-Frag workflow. Unanticipated modifications outside this list would not be detected, and the expanded search space increases false-positive risk despite FDR correction. Isobaric ambiguities such as trimethylation (+42.047 Da) vs acetylation (+42.011 Da) require high mass accuracy for confident discrimination, and some site assignments may remain probabilistic for peptides with multiple closely spaced modifiable residues. Notably, however, the RIPUP protocol is compatible with

open-search pipelines for PTM discovery, so these constraints exist in downstream analysis rather than in the protocol itself.

Following Vai et al. [15], we relied on stringent computational filtering rather than synthetic peptide validation for most PTMs identified, and propionylation efficiency was not validated against synthetic standards. TMT was employed exclusively as a derivatization agent, its multiplexing and quantitative capabilities were not utilized, and enhanced succinylation/glutarylation detection likely reflects improved ionization rather than absolute abundance differences. Finally, endogenous propionylation and butyrylation cannot be distinguished from chemical derivatization artifacts in propionylated samples, a limitation the RIPUP workflow circumvents by omitting chemical derivatization.

Conclusions

We present RIPUP, a rapid multi-protease workflow that reduces histone PTM sample preparation from days to hours while expanding PTM coverage through strategic use of complementary proteases. Our systematic evaluation of Arg-C Ultra and r-Chymotrypsin across 40 samples spanning 10 conditions provides a detailed roadmap for method optimization. We confirm that Arg-C Ultra achieves superior digestion specificity compared to conventional Arg-C and extend recent findings by demonstrating that TMT labeling offers unique advantages over TMA derivatization [9]. Specifically, TMT's tertiary amine provides charge compensation that rescues ionization of acidic acylations, revealing 50 succinylation and 27 glutarylation sites constituting an otherwise hidden 'dark epigenome'. This finding suggests the biological prevalence of negatively charged PTMs has been systematically underestimated with conventional propionylation-based workflows.

Application to rat hippocampal tissue confirmed detection of 231 unique PTM sites including biologically critical marks within a three-hour sample preparation window. For method selection, RIPUP with TMT labeling is optimal when acidic acylations are of interest, when multiplexing is desired, or when rapid turnaround is essential. TMA-based approaches may offer advantages for certain positional isomer separations, and complementary r-Chymotrypsin digestion should be included when comprehensive coverage of H2A variants and linker histones is required. Collectively, these methods expand the analytical toolkit for histone PTM research and should facilitate higher-throughput epigenetic studies where rapid, comprehensive profiling is essential for accelerating therapeutic discovery and mechanistic understanding.

Supporting information

Supplementary information is available as follows; File 1, Figure S1: Trypsin and TMT-labeled HEK293T comparisons (CVs, peptide length distributions, missed cleavages, histone protein sequence coverage, artifact rates), and cleavage specificity (R vs KR) for trypsin groups. Figure S2: H1.4 sequence coverage and succinylation sites in r-Chymotrypsin + TMT and Arg-C Ultra + TMT samples. Figure S3: H4 sequence coverage and succinylation sites in r-Chymotrypsin + TMT samples and fragment spectra for RDNIQGITkPAIRRL and ARRGGVkRISGL peptides. Figure S4: H4 sequence coverage and succinylation sites in Arg-C Ultra + TMT samples and fragment spectra for DNIQGITkPAIR and DAVTYTEHAkR peptides. Figure S5: Unique peptidoforms and CVs of histones extracted from rat hippocampal sections that underwent the RIPUP protocol. File 2: SDS-PAGE image files. File 3: Peptide lists of modified peptides identified in Rat hippocampal sections using the RIPUP workflow (Arg-C Ultra and r-Chymotrypsin).

Data availability

The MS raw data files, annotations, Sample and Data Relationship Format (SDRF-Proteomics)[52], and FragPipe search have been deposited to the ProteomeXchange Consortium (http://proteomecentral.proteomexchange.org) [53,54] via the PRIDE partner repository [55] with the dataset identifier PXD073683. The custom R scripts used for data analysis are available at: https://github.com/NataliePTurner/Histone-RIPUP

Acknowledgements

Support for this study was provided by National Institute on Alcohol Abuse and Alcoholism grants: T32 AA007456, AA013498 (MR, MB), P60 AA006420 (MR, JY), AA017447 (MR), AA029841 (MR), AA021491 (MR) and the Schimmel Family Chair.

References

1. Sidoli, S., Bhanu, N. V., Karch, K. R., Wang, X. & Garcia, B. A. Complete workflow for analysis of histone post-translational modifications using bottom-up mass spectrometry: From histone extraction to data analysis. *Journal of Visualized Experiments* **2016**, (2016).

2. Garcia, B. A. *et al.* Chemical derivatization of histones for facilitated analysis by mass spectrometry. *Nat. Protoc.* **2**, 933–938 (2007).

3. Amatori, S., Tavolaro, S., Gambardella, S. & Fanelli, M. The dark side of histones: genomic organization and role of oncohistones in cancer. *Clinical Epigenetics* vol. 13 Preprint at https://doi.org/10.1186/s13148-021-01057-x (2021).

4. Park, J., Lee, K., Kim, K. & Yi, S. J. The role of histone modifications: from neurodevelopment to neurodiseases. *Signal Transduction and Targeted Therapy* vol. 7 Preprint at https://doi.org/10.1038/s41392-022-01078-9 (2022).

5. Jordi, E. *et al.* Differential effects of cocaine on histone posttranslational modifications in identified populations of striatal neurons. *Proc. Natl. Acad. Sci. U. S. A.* **110**, 9511–9516 (2013).

6. Lund, P. J. *et al.* Stable isotope tracing in vivo reveals a metabolic bridge linking the microbiota to host histone acetylation. *Cell Rep.* **41**, 111809 (2022).

7. Sidoli, S., Bhanu, N. V., Karch, K. R., Wang, X. & Garcia, B. A. Complete workflow for analysis of histone post-translational modifications using bottom-up mass spectrometry: From histone extraction to data analysis. *Journal of Visualized Experiments* **2016**, (2016).

8. Searfoss, R. M., Karki, R., Lin, Z., Robison, F. & Garcia, B. A. An Optimized and High-Throughput Method for Histone Propionylation and Data-Independent Acquisition Analysis for the Identification and Quantification of Histone Post-translational Modifications. *J. Am. Soc. Mass Spectrom.* **34**, 2508–2517 (2023).

9. Ryzhaya, P., Pírek, P., Zdráhal, Z. & Lochmanová, G. Arg-C Ultra Simplifies Histone Preparation for LC-MS/MS. *Anal. Chem.* **97**, 12486–12492 (2025).

10. Sidoli, S. *et al.* One minute analysis of 200 histone posttranslational modifications by direct injection mass spectrometry. *Genome Res.* **29**, 978–987 (2019).

11. Meert, P., Govaert, E., Scheerlinck, E., Dhaenens, M. & Deforce, D. Pitfalls in histone propionylation during bottom-up mass spectrometry analysis. *Proteomics* **15**, 2966–2971 (2015).

12. Thompson, A. *et al.* Tandem Mass Tags: A Novel Quantification Strategy for Comparative Analysis of Complex Protein Mixtures by MS/MS. *Anal. Chem.* **75**, 1895–1904 (2003).

13. Zhang, Z. *et al.* Identification of lysine succinylation as a new post-translational modification. *Nat. Chem. Biol.* **7**, 58–63 (2011).

14. Weyh, M., Jokisch, M.-L., Nguyen, T.-A., Fottner, M. & Lang, K. Deciphering functional roles of protein succinylation and glutarylation using genetic code expansion. *Nat. Chem.* **16**, 913–921 (2024).

15. Vai, A. *et al.* Breaking Boundaries in Histone Modification MS-Based Detection: A Tailored Search Strategy for Unrestricted Identification of Novel Epigenetic Marks. *Molecular & Cellular Proteomics* **24**, 101080 (2025).

16. Vozella, V. *et al.* Apremilast reduces co-occurring alcohol drinking and mechanical allodynia and regulates central amygdala GABAergic transmission. *JCI Insight* **10**, (2025).

17. Guo, Y. *et al.* Scalable total synthesis of saxitoxin and related natural products. *Nature* **646**, 351–357 (2025).

18. Diedrich, J. K., Pinto, A. F. M. & Yates, J. R. Energy Dependence of HCD on Peptide Fragmentation: Stepped Collisional Energy Finds the Sweet Spot. *J. Am. Soc. Mass Spectrom.* **24**, 1690–1699 (2013).

19. Vai, A. *et al.* Improved Mass Spectrometry–Based Methods Reveal Abundant Propionylation and Tissue-Specific Histone Propionylation Profiles. *Molecular & Cellular Proteomics* **23**, 100799 (2024).

20. Fu, Z., Akula, S., Thorpe, M. & Hellman, L. Marked difference in efficiency of the digestive enzymes pepsin, trypsin, chymotrypsin, and pancreatic elastase to cleave tightly folded proteins. *Biol. Chem.* **402**, 861–867 (2021).

21. Paizs, B. & Suhai, S. Fragmentation pathways of protonated peptides. *Mass Spectrom. Rev.* **24**, 508–548 (2005).

22. Steen, H. & Mann, M. The abc's (and xyz's) of peptide sequencing. *Nat. Rev. Mol. Cell Biol.* **5**, 699–711 (2004).

23. Thomas, S. P., Haws, S. A., Borth, L. E. & Denu, J. M. A practical guide for analysis of histone post-translational modifications by mass spectrometry: Best practices and pitfalls. *Methods* **184**, 53–60 (2020).

24. Maile, T. M. *et al.* Mass Spectrometric Quantification of Histone Post-translational Modifications by a Hybrid Chemical Labeling Method. *Molecular & Cellular Proteomics* **14**, 1148–1158 (2015).

25. Whedon, S. D. *et al.* Circular Engineered Sortase for Interrogating Histone H3 in Chromatin. *J. Am. Chem. Soc.* **146**, 33914–33927 (2024).

26. Challa, K. *et al.* Damage-induced chromatome dynamics link Ubiquitin ligase and proteasome recruitment to histone loss and efficient DNA repair. *Mol. Cell* **81**, 811-829.e6 (2021).

27. Xie, Z. *et al.* Lysine Succinylation and Lysine Malonylation in Histones. *Molecular & Cellular Proteomics* **11**, 100–107 (2012).

28. Liu, J., Shangguan, Y., Tang, D. & Dai, Y. Histone succinylation and its function on the nucleosome. *Journal of Cellular and Molecular Medicine* vol. 25 7101–7109 Preprint at https://doi.org/10.1111/jcmm.16676 (2021).

29. Zorro Shahidian, L. *et al.* Succinylation of H3K122 destabilizes nucleosomes and enhances transcription. *EMBO Rep.* **22**, (2021).

30. Jing, Y. *et al.* Semisynthesis of site-specifically succinylated histone reveals that succinylation regulates nucleosome unwrapping rate and DNA accessibility. *Nucleic Acids Res.* **48**, 9538–9549 (2020).

31. Bao, X. *et al.* Glutarylation of Histone H4 Lysine 91 Regulates Chromatin Dynamics. *Mol. Cell* **76**, 660-675.e9 (2019).

32. Stransky, S. *et al.* Preliminary Evidence for Increased Histone Succinylation as a Potential Epigenetic Marker for Longevity. *Aging Cell* **25**, (2026).

33. Tan, M. *et al.* Lysine Glutarylation Is a Protein Posttranslational Modification Regulated by SIRT5. *Cell Metab.* **19**, 605–617 (2014).

34. Bao, X. *et al.* Glutarylation of Histone H4 Lysine 91 Regulates Chromatin Dynamics. *Mol. Cell* **76**, 660-675.e9 (2019).

35. Li, J. *et al.* A Novel Histone H4 Arginine 3 Methylation-sensitive Histone H4 Binding Activity and Transcriptional Regulatory Function for Signal Recognition Particle Subunits SRP68 and SRP72. *Journal of Biological Chemistry* **287**, 40641–40651 (2012).

36. Feng, Y. *et al.* Histone H4 Acetylation Differentially Modulates Arginine Methylation by an in Cis Mechanism. *Journal of Biological Chemistry* **286**, 20323–20334 (2011).

37. Schiza, V., Molina-Serrano, D., Kyriakou, D., Hadjiantoniou, A. & Kirmizis, A. N-alpha-terminal Acetylation of Histone H4 Regulates Arginine Methylation and Ribosomal DNA Silencing. *PLoS Genet.* **9**, e1003805 (2013).

38. Pessoa Rodrigues, C. *et al.* Histone H4 lysine 16 acetylation controls central carbon metabolism and diet-induced obesity in mice. *Nat. Commun.* **12**, 6212 (2021).

39. Shogren-Knaak, M. *et al.* Histone H4-K16 Acetylation Controls Chromatin Structure and Protein Interactions. *Science (1979).* **311**, 844–847 (2006).

40. Renthal, W. & Nestler, E. J. Histone acetylation in drug addiction. *Semin. Cell Dev. Biol.* **20**, 387–394 (2009).

41. Cao, R. *et al.* Role of Histone H3 Lysine 27 Methylation in Polycomb-Group Silencing. *Science (1979).* **298**, 1039–1043 (2002).

42. Salzler, H. R. *et al.* Distinct roles for canonical and variant histone H3 lysine-36 in Polycomb silencing. *Sci. Adv.* **9**, (2023).

43. Zheng, Y. *et al.* Total kinetic analysis reveals how combinatorial methylation patterns are established on lysines 27 and 36 of histone H3. *Proceedings of the National Academy of Sciences* **109**, 13549–13554 (2012).

44. Sparmann, A. & Van Lohuizen, M. Polycomb silencers control cell fate, development and cancer. *Nature Reviews Cancer* vol. 6 846–856 Preprint at https://doi.org/10.1038/nrc1991 (2006).

45. Zheng, S. & Doucette, A. A. Preventing *N* - and *O* -formylation of proteins when incubated in concentrated formic acid. *Proteomics* **16**, 1059–1068 (2016).

46. Wiśniewski, J. R., Zougman, A. & Mann, M. N ε -Formylation of lysine is a widespread post-translational modification of nuclear proteins occurring at residues involved in regulation of chromatin function. *Nucleic Acids Res.* **36**, 570–577 (2008).

47. Jiang, T., Zhou, X., Taghizadeh, K., Dong, M. & Dedon, P. C. N-formylation of lysine in histone proteins as a secondary modification arising from oxidative DNA damage. *Proceedings of the National Academy of Sciences* **104**, 60–65 (2007).

48. Wiśniewski, J. R., Zougman, A., Krüger, S. & Mann, M. Mass Spectrometric Mapping of Linker Histone H1 Variants Reveals Multiple Acetylations, Methylations, and Phosphorylation as Well as Differences between Cell Culture and Tissue. *Molecular & Cellular Proteomics* **6**, 72–87 (2007).

49. Nardiello, D., Palermo, C., Natale, A., Quinto, M. & Centonze, D. Strategies in protein sequencing and characterization: Multi-enzyme digestion coupled with alternate CID/ETD tandem mass spectrometry. *Anal. Chim. Acta* **854**, 106–117 (2015).

50. Swaney, D. L., Wenger, C. D. & Coon, J. J. Value of Using Multiple Proteases for Large-Scale Mass Spectrometry-Based Proteomics. *J. Proteome Res.* **9**, 1323–1329 (2010).

51. MacCoss, M. J. *et al.* Shotgun identification of protein modifications from protein complexes and lens tissue. *Proceedings of the National Academy of Sciences* **99**, 7900–7905 (2002).

52. Dai, C. *et al.* A proteomics sample metadata representation for multiomics integration and big data analysis. *Nat. Commun.* **12**, 5854 (2021).

53. Deutsch, E. W. *et al.* The ProteomeXchange consortium in 2026: making proteomics data FAIR. *Nucleic Acids Res.* https://doi.org/10.1093/nar/gkaf1146 (2025) doi:10.1093/nar/gkaf1146.

54. Deutsch, E. W. *et al.* The ProteomeXchange consortium in 2017: supporting the cultural change in proteomics public data deposition. *Nucleic Acids Res.* **45**, D1100–D1106 (2017).

55. Perez-Riverol, Y. *et al.* The PRIDE database at 20 years: 2025 update. *Nucleic Acids Res.* **53**, D543–D553 (2025).